

# Performance of Construction with New Pneumatic Caisson Method in Shanghai Soft Ground

F. L. Peng<sup>1,2</sup>, H. L. Wang<sup>1</sup>

<sup>1</sup>Department of Geotechnical Engineering, Tongji University, Shanghai, P.R.China

<sup>2</sup>Key Laboratory of Geotechnical and Underground Engineering, Ministry of Education, P.R.China

Email: pengfangle@tongji.edu.cn

**ABSTRACT:** In the new pneumatic caisson method (NPC), soil excavation and removal is completed remotely by workers on the ground. In 2007, this method was successfully applied in a tunnel shaft in Shanghai. Combined with the construction example, field monitoring and measuring has been conducted. Typical monitored results, such as the working pressure, lateral earth pressure, reaction pressure, and ground movements, were presented and analyzed. In addition, a numerical approach considering the soil disturbance during construction was proposed to predict the soil movements induced by the NPC construction. It was successfully implemented in the three-dimensional finite element method (FEM) codes. Calculated soil movements were examined and verified by the field measurements. In the meantime, these results were compared with the ones obtained from the two-dimensional approach proposed by the authors in the previous study. Results showed that, they agreed well with each other, and in general the three-dimensional analysis results approached the actual situation more closely.

## 1. INTRODUCTION

The pneumatic caissons are similar to open caissons, but sealed at the bottom to create a working chamber. Soils are excavated in the chamber, and the groundwater is kept outside by the compressed air inside. In the traditional pneumatic caissons, workers have to conduct excavation inside the working chamber under high pressures, high temperatures, and high humidity. While in the new pneumatic caissons (NPC), soil excavation and removal is completed by the remotely controlled equipments. This method is applicable to various ground conditions. Moreover, it allows the excavation face to be video-monitored directly and improves the safety for its unmanned work. The pressure of the compressed air inside the working chamber can prevent the ground water from inflowing, stabilize the groundwater table, and hence minimize the disturbances to the environment. Therefore, it has been regarded as one safe and effective underground excavation method.

Pneumatic caissons have been constructed in many countries and regions, especially in Japan. The advanced automatic system for the pneumatic caisson construction has been developed and put into practice (Kodaki et al. 1997). In China, there are some traditional pneumatic caissons completed many years ago. In 2007, the NPC method was applied to construct one tunnel shaft in Shanghai, China for the first time. Preliminary studies referring to its environmental impacts have been conducted (Peng et al. 2009). With its wider application of the NPC method, more and more deep excavations have been/will be constructed in the sensitive and unstable soft ground, which results in sharply increasing risks and adverse impacts on the environment. To ensure the construction accuracy and safety, field monitoring and measuring is an indispensable procedure. It is also essential to the remote-control work by the use of captured videos and monitored environmental parameters in the working chamber. Besides, it is of vital importance to investigate and predict its impacts on the surrounding strata and adjacent structures during the process of the caisson sinking. The authors have proposed a kinematic mechanical model for evaluating the ground deformation induced by the NPC construction in the previous study (Peng et al. 2011). This model was incorporated into a two-dimensional finite element program. Its accuracy and reliability were verified through comparison of the calculated results with the field measurements. However, in this analysis model the caisson structure itself was not taken into account; neither were the three-dimensional effects of the practical problems. Furthermore, soils around the caisson were subjected to repeated disturbances during the caisson sinking, mainly because of the skin-friction drag of the caisson walls and extruding of the cutting edge.

Unfortunately, this fact was not considered in the two-dimensional analysis.

In this study, combined with a shaft construction using the NPC method, typical monitored results at the site were analyzed. The purposes of this study are to summarize the field instrumentation for the NPC construction, interpret the field measured results, and propose a three-dimensional FEM approach considering the soil disturbance to predict the ground movements induced by the NPC construction.

## 2. TUNNEL SHAFT CONSTRUCTED BY THE NPC METHOD

The completed vertical tunnel shaft was located about 56.0 m away from Huangpu River. According to the site exploration results, the subsoil at the site consisted of silt of low plasticity (ML) in the upper 7.5 m below the ground surface (BGS), followed by clay of high plasticity (CH) to a depth of 13.5 m BGS. Directly below the CH layer, silt of low plasticity (ML) was encountered to a depth of 24.0 m BGS, underneath by clay (CL) till the termination of the field exploration. The ground water table was located at 0.5 to 1.0 m BGS. Figure 1 shows the transverse profile of the shaft and soil conditions, in which the soil properties are listed including the unit weight  $\gamma$ , cohesion  $c$ , friction angle  $\varphi$ , water content  $\omega_w$ , and liquid limit LL.

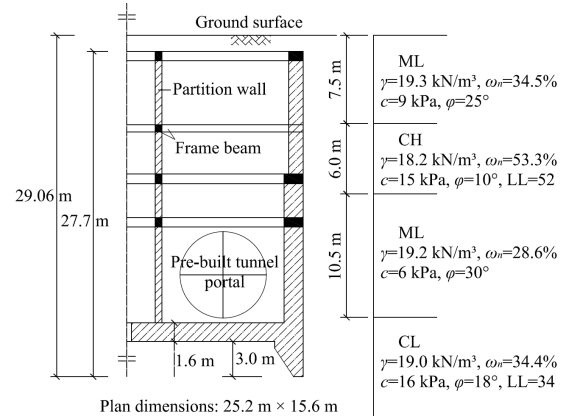


Figure 1 Transverse profile of the shaft and soil conditions

The shaft construction to be presented in this study was one part of the shield tunneling project of Metro Line 7 in Shanghai, which would be used as a shield work shaft initially and as a ventilation

shaft while in operation. This shaft was completed by the NPC method, which was the first time to be used in China. The shaft was a fully embedded reinforced concrete caisson with the external dimensions of 25.2 m (length)  $\times$  15.6 m (width)  $\times$  27.7 m (height), which included a working chamber. Its total sinking depth was around 29.06 m. Pre-built tunnel portals were made for the shield launching or arrival and the outer wall of the caisson was configured with no friction cut. In addition, two vertical partition walls were installed in the transverse direction and one in the longitude direction, creating several compartments.

In this project, the caisson shaft was built in six segments on the ground surface. First, eight anchor piles around each corner of the caisson were cast in place, which were used to aid caisson sinking; second, one shallow excavation of about 4.0 m deep was made for the treatment of shallow ground such as sand replacement; third, a working chamber, including the cutting edge and ceiling slab, was cast and then construction equipments for the NPC (e.g., caisson excavators and manlocks) were attached to the ceiling slab; finally, caisson fabrication continued. When the first three segments (a total of 7.6 m high) were made the caisson sunk by 3.0 m. In the following, the caisson sunk in three phases (i.e. after the caisson was extended by the segment each time, the sinking began). Depths of sinking in each phase were 4.20 m, 8.80 m, and 10.06 m, respectively. Figure 2 shows the NPC under construction. From Phase 2, compressed air was pumped into the working chamber from the air-generators. The air pressures were instantly and automatically adjusted according to the groundwater level in the chamber.



Figure 2 NPC under construction

During the construction, all the work of soil excavation and removal was done by the remotely controlled system. Sitting in the control room on the ground surface, the construction workers manipulated the handles to operate the caisson excavators and other devices easily and comfortably, just gazing on the screen videos captured in real-time by the cameras installed in the working chamber. The construction started in Nov., 2006 and ended in Oct., 2007. The total time spent on caisson sinking were 133 days, and an average sinking depth of 20 cm per day was achieved.

### 3. SITE MONITORING AND PERFORMANCE

#### 3.1 Field Instrumentation

Monitored items for the NPC mainly included the following aspects: a) geometrical parameters of the caisson, such as the plan and depth position of the caisson, sinking rate, tilting rate, and so on; b) mechanical behavior of the caisson structure, referring to loads, internal forces, and deformation; c) environmental impacts caused by the construction (e.g. the ground water table, deformations of surrounding soils, buildings and pipelines). In particular, air leakage from the working chamber should be checked; d) environmental parameters in the working chamber (e.g. air ingredients, pressures, and temperature). The last aspect was unique and essential to the NPC construction, compared to other commonly used braced

excavation methods. Monitored data could be acquired automatically or manually. The typical field instrumentation in the NPC is shown in Figure 3. To be noted that, in the construction example mentioned above, the caisson tilting was measured by the elevation differences of the four caisson corners. The skin friction was obtained based on the measured lateral earth pressure and the friction factor between the caisson wall and soils. In addition, as required by the remote excavation, some cameras and laser scanners were installed in the working chamber. Thus, conditions of the ground and excavators were under surveillance in real-time, by videos or digital display on the monitoring screen (Li et al. 2010).

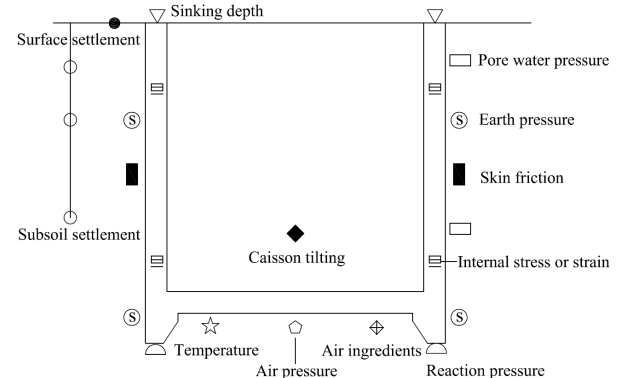


Figure 3 Profile of field instrumentation in the NPC

#### 3.2 Monitored results of the caisson shaft construction

In the above mentioned caisson construction project, site monitoring was conducted through the caisson sinking process. In this section, selected monitored results, ever reported by Wang et al. (2011), will be analyzed.

##### 3.2.1 Working Pressure

The working pressure in the working chamber was adjusted accordingly with the progress of caisson sinking. The recorded values of the pressure with respect to the construction time are plotted in Figure 4, in which the sinking depth of the caisson is also incorporated.

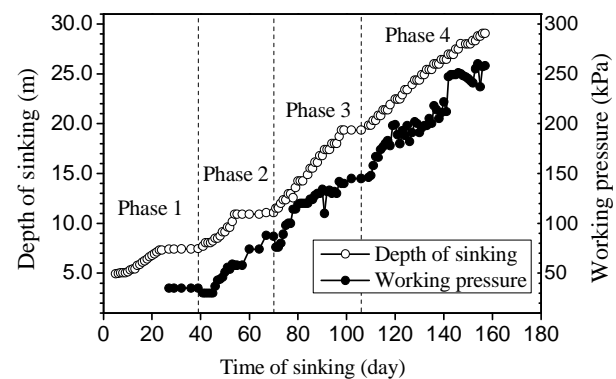


Figure 4 Working pressure and depth of sinking

From the graph we can see that, the working pressure grew linearly with the sinking depth. The compressed air pressure was set about 32 kPa smaller than the theoretical pore water pressure at the caisson base. For the soft clay in Shanghai, the actual pore water pressure could be considered significantly lower than the estimated static water pressure because of low permeability of clay, which was consistent with field measurement results (Liu et al. 2000).

### 3.2.2 Lateral Earth Pressure on the Caisson Wall

In the NPC construction, a total of 14 earth pressure cells were installed along the depth direction to investigate the lateral earth pressures on the caisson wall. On the short edge of the caisson, seven cells were placed denoted as from CP11 to CP17, of which CP13 was damaged by the construction in the third sinking phase; while on the long edge, four of seven cells were damaged. Therefore, layout of the cells and measured results on the short edge are presented in Figure 5. As shown in the graph, the pressures of installed CP11, CP12, and CP13 varied little in the first phase. However, in the following phases, pressures of all cells increased with the sinking progress. The pressure of CP11, located close to the cutting edge, was the maximum of all monitored pressures and finally reached 284 kPa.

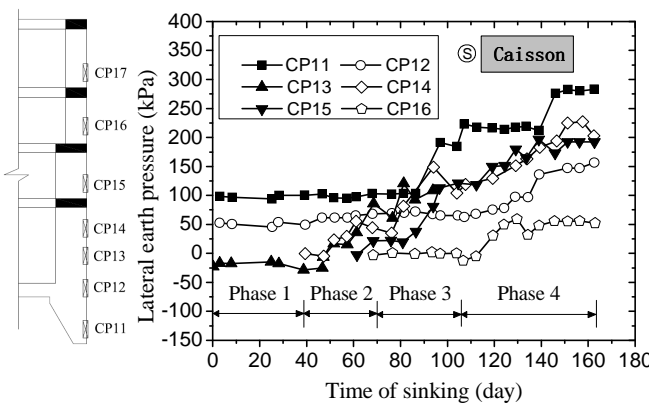


Figure 5 Lateral pressures on the caisson wall

### 3.2.3 Reaction Pressure on the Cutting Edge

At the caisson base, a total of ten earth pressure cells were installed beneath the cutting edge denoted as from SP01 to SP10, to obtain the upward reaction pressures on the cutting edge. Some typical monitored data are plotted in Figure 6, in which the relative locations of each cell are also added.

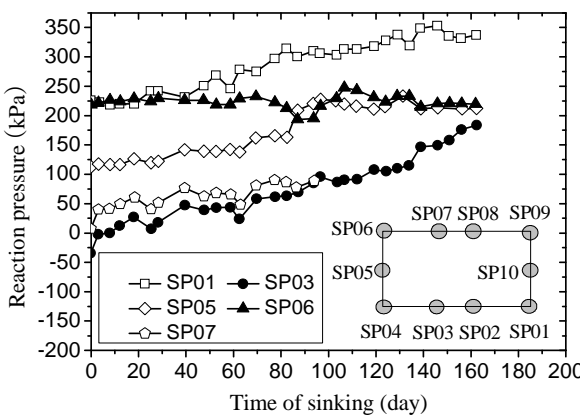


Figure 6 Reaction pressures on the cutting edge

According to the graph, the reaction pressures at SP01 and SP07 were larger than those at other cells. Pressures at SP03 and SP07 were the smallest, and the pressure at SP05 ranked in the middle. Thus, the reaction pressures on the cutting edge were not distributed uniformly and significant spatial effects existed. The reaction pressures at the caisson corner were biggest, followed by those in the middle of the short edge, then in the middle of the long edge. The pressures of SP01 and SP06 (both at the caisson corner) were close initially; however, in the following, the pressure of SP01 increased gradually, while the pressure of SP06 remained the same and even decreased. This phenomenon could be attributed to that, the reaction pressure distribution was easily affected by the

nonhomogeneity of ground and uncertainties of the construction control.

To be noted that, the pressure of SP03 initially was below zero, and then increased with the caisson sinking. In the initial stage, because of shrinkage of concrete cutting edge, the pressure cell was not closely in contact with the caisson, and thus a negative earth pressure was recorded. With the construction progress, the caisson pressured the cell and the positive pressure was recorded.

### 3.2.4 Ground Movement Around the Caisson

To investigate the impacts of the NPC construction on the environment, some monitoring points or vertical boreholes were laid out around the caisson before caisson sinking. The layout of the in-situ measurement is shown in Figure 7. The monitoring points for surface settlements (designated as D) were arranged at increments of 5.0 m away from the caisson wall, in four directions from D1 to D4. These points were surveyed by total station instruments. The boreholes (designated as T) were 35.0 m deep, in which inclinometer casings were installed for measuring subsurface horizontal movements.

Observed data at the surveyed points or boreholes are shown in Figures 8 and 9. For simplicity, some data are omitted, for they show similar values or trends.

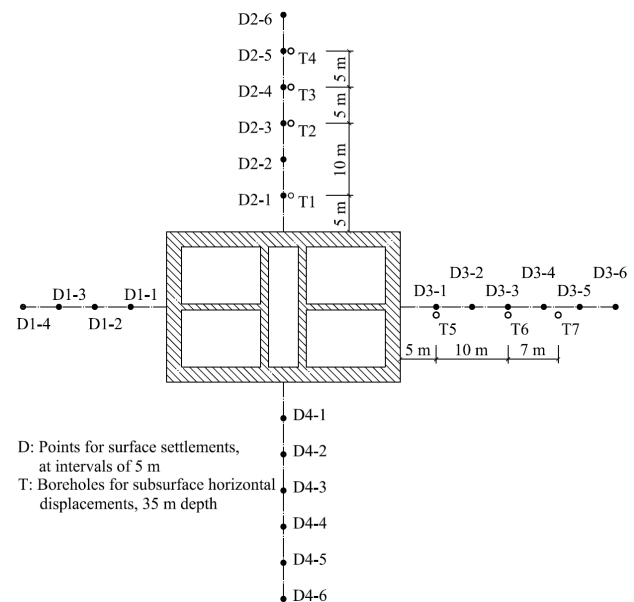
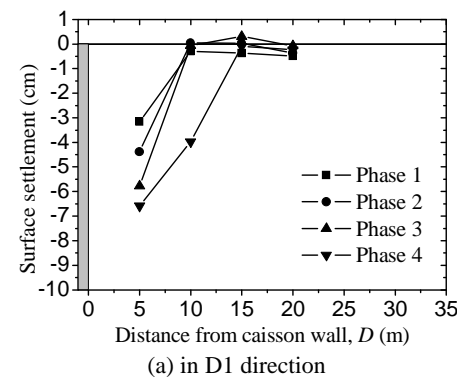
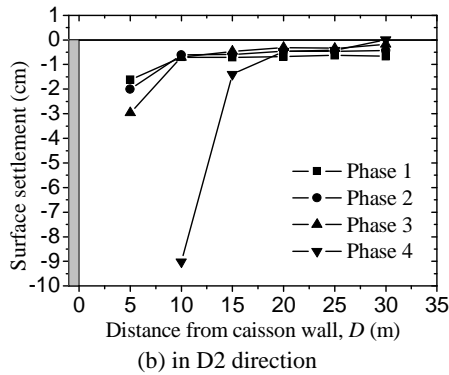


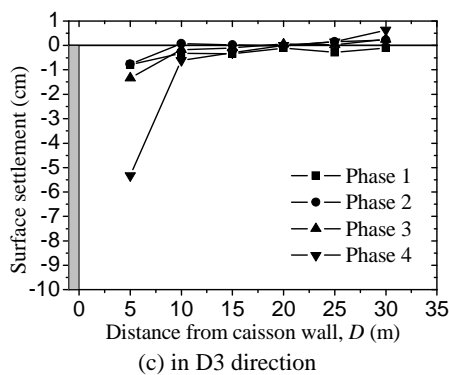
Figure 7 Layout of the surveyed locations



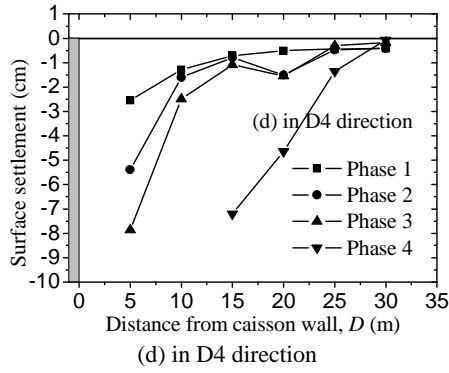
(a) in D1 direction



(b) in D2 direction

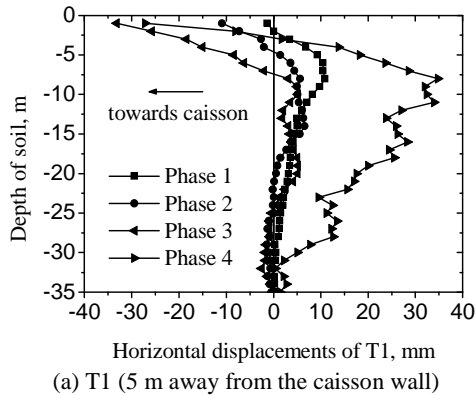


(c) in D3 direction

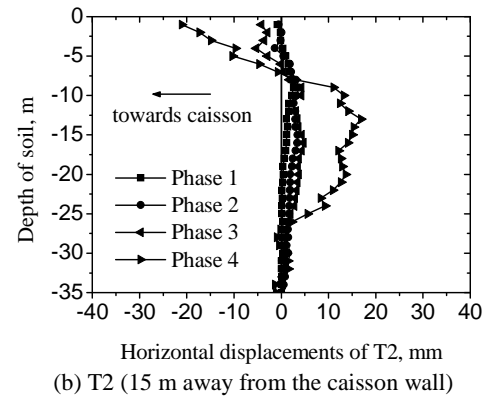


(d) in D4 direction

Figure 8 Measured surface settlements



(a) T1 (5 m away from the caisson wall)



(b) T2 (15 m away from the caisson wall)

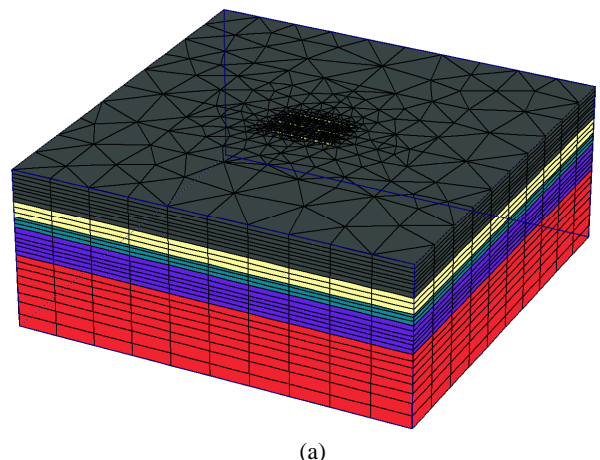
Figure 9 Measured subsoil horizontal displacements

From these graphs, it can be observed that the caisson construction caused very small soil movements in the first three sinking phase. Within the areas from 5.0 m to 10.0 m away from the caisson wall, the surface settlements decreased significantly. Beyond 10.0 m from the caisson wall, the construction had very limited impacts on the ground settlements, and the measured settlements were no more than 30 mm. Most of the subsurface horizontal movements at the boreholes were negligible, no more than 10 mm. However, in the last sinking phase the measured values increased dramatically, and even some measured points around the caisson were damaged by excessive settlements. The greater sinking depth in one phase, easily leading to greater soil horizontal movements due to caisson tilting, might attribute to the relatively large ground deformation. Fortunately, its adjacent buildings and pipe lines were free from damage.

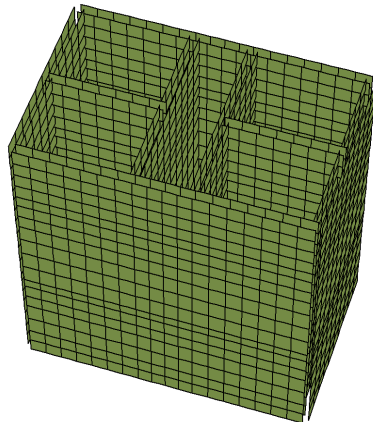
#### 4. THREE DIMENSIONAL NUMERICAL ANALYSES OF THE NPC CONSTRUCTION

##### 4.1 Calculation Model and Simulation Techniques

The three-dimensional numerical analysis was implemented in the commercial finite element analysis program Plaxis 3D Foundation. A three-dimensional calculation model, with a size of 150 m  $\times$  150 m  $\times$  60 m, was established to simulate the whole NPC construction progress. In this model, the caisson structure (25.2 m  $\times$  15.6 m  $\times$  29.0 m) and its surrounding strata were incorporated. The size of the calculation region was determined from the experience of open caissons construction. Its finite element mesh is shown in Figure 10 (a). The soil elements to be "excavated" were also included in the mesh. The basic soil elements adopted in this model were the 15-node wedge elements. In addition, 6-node and 8-node plate elements were used to simulate the behavior of the caisson walls and slabs. Moreover, 12-node and 16-node interface elements were used to simulate the interaction behavior between the caisson wall and its surrounding soils, as shown in Figure 10 (b).



(a)



(b)

Figure 10 The 3D calculation model and its interface elements

Therefore, in the three-dimensional numerical analysis, the stress-strain state of the caisson and soils, and the interaction between them could be obtained. To simplify the analysis, the horizontal displacement and tilting of the caisson were not taken into account in this model. Besides, the ground water seepage was considered small enough and neglected because of existence of the compressed air.

In the FE analyses, firstly the initial stresses of the entire stratum, assumed to be normally consolidated, were generated by using gravity loading. Herein, the coefficient of lateral earth pressure at rest  $K_0$  was determined from Jaky's formula  $K_0 = 1 - \sin \phi$ . Afterwards, the caisson sinking process was modeled by four continuous phases based on the construction records. For simplification, the shallow excavation and the following sand replacement in the initial period were not taken into account. Thus the sinking depth in the first phase was defined as 6.0 m. The depths in the following three phases were 10.2 m, 19.0 m, 29.0 m, respectively. In each phase, corresponding "excavated" soil elements were deactivated, and structure elements along with the interface elements were activated in the phase definition. In the program the stiffness and weight of the deactivated soil elements were automatically set to a value of approximate zero in the calculation and thus the state of stress of the same elements was also reduced to zero by the application of equivalent nodal forces to the surrounding nodes. Also, the steady state pore pressures in these elements were set to zero, but the phreatic level remained the same, taking the air pressures into account.

The numerical analysis was carried out in terms of effective stresses. In PLAXIS 3D Foundation, it was possible to specify undrained behavior in an effective stress analysis using effective model parameters. This was achieved by identifying the type of material behavior of a soil layer as undrained. Detailed information on the special option could be found in the PLAXIS 3D Foundation Material Models Manual. Thus, the short-term behavior of soils during construction could be well simulated.

#### 4.2 Model Parameters Considering Soil Disturbance

Unlike other commonly used braced excavation methods such as the diaphragm, the caisson structure was always in motion during the NPC construction, and soils around the caisson were subjected to more intense disturbance. Generally, there were mainly three types of disturbed soils, including unloading zone, compacted zone and shear zone (see Figure 11).

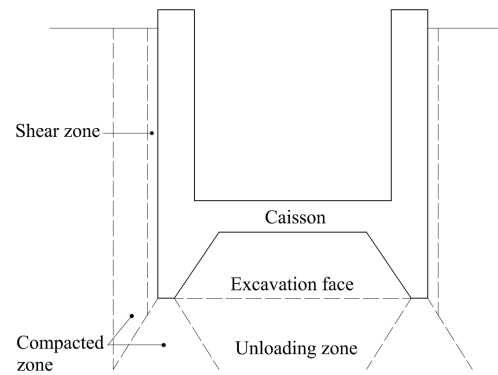


Figure 11 Disturbed soils around the caisson

Obviously, the unloading zone formed as a result of excavation of soils above. The compacted zone consisted of soils being (or had ever been) extruded by the caisson cutting edge. The shear zone was induced by the skin-friction drag of the caisson wall. In the following, effects of these disturbances would be taken into account in the numerical analysis by adoption of modified model or parameter values.

Due to unloading, soils beneath the caisson behaved differently from them before excavation. To model the soil behavior more accurately, the advanced elasto-plastic constitutive model Hardening-Soil (HS) model was employed. The HS model has the ability to simulate the advanced behaviors of many soils including soft and hard soils. According to the test results, the material parameters of drained type used in this analysis are summarized in Table 1, in which  $E_{50}^{\text{ref}}$  is the reference stiffness modulus corresponding to the reference confining pressure  $p^{\text{ref}}$ , and  $E_{ur}^{\text{ref}}$  is the reference Young's modulus for un-/reloading (Schanz et al. 1999). According to the laboratory test results, the dilatancy behavior of soils at the site was not observed, and hence the dilatancy angle was set to zero for all the soils.

In the compacted zone, the soil density was significantly increased, which was associated with increased stiffness. Laboratory test results showed that, the compression index  $C_c$  of remoulded soft clay in Shanghai was approximately 23% - 40% smaller than that of the undisturbed soils (Chen 2008). Thus, to consider the compaction effects, in the model a soil-compacted ring-wall closely around the caisson was designated by an increase of 30% of soil modulus (i.e.  $E_{50}^{\text{ref}}$  and  $E_{ur}^{\text{ref}}$ ) within this ring, as shown in Figure 12. It was assumed that, the influence depth of soil compaction was located where the additional stress was 20% of the reaction pressure under the cutting edge. In addition, considering that the addition stress due to the caisson self-weight spread downwards at a 45-degree angle, the width of the ring was set to twice that of the caisson cutting edge, i.e. 2.4 m. Its height in depth approximately equaled to the sinking depth from the ground surface, updated with the progress of caisson sinking in each phase.

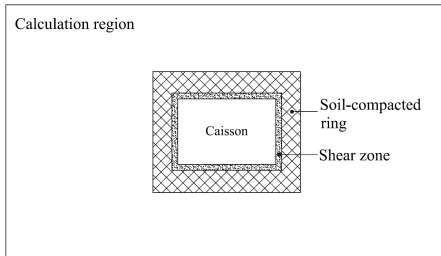


Figure 12 Plan view of the disturbed soils

As mentioned previously, interfaces between the structure and its surrounding soils were designated at both sides of the caisson wall in the calculation model, to consider the disturbance of soils in the shear zone. In PLAXIS 3D Foundation, the interfaces are mainly composed of interface elements of eight pairs of nodes, compatible with the 8-noded quadrilateral side of a soil element. Along the degenerated soil elements, interface elements are composed of 6 node pairs, compatible with the triangular side of the degenerated soil element. The strength properties of interfaces are linked to the strength properties of a soil layer. Each soil data set has an associated strength reduction factor for interfaces  $R_{\text{inter}}$ . The interface properties are calculated from the soil properties in the associated data set and the strength reduction factor by applying the following rules:

Table 1 Soil Parameters used in the FEM Analyses

Layers of soil	Submerged unit weight $\gamma'$ (kN/m <sup>3</sup> )	Cohesion $c$ (kN/m <sup>2</sup> )	Friction angle $\phi$ (°)	Poisson's ratio $\nu_{ur}$	Dilatancy angle $\psi$ (°)	$E_{50}^{\text{ref}}$ (kN/m <sup>2</sup> )	$E_{ur}^{\text{ref}}$ (kN/m <sup>2</sup> )	$p^{\text{ref}}$ (kPa)
ML	9.3	9	25	0.2	0	17940	71760	100.0
CH	8.2	15	10	0.2	0	6030	24120	100.0
ML	9.2	6	30	0.2	0	24000	96000	100.0
CL	9.0	16	18	0.2	0	10320	41280	100.0

$$\left. \begin{aligned} c_i &= R_{\text{inter}} c_{\text{soil}} \\ \tan \phi_i &= R_{\text{inter}} \tan \phi_{\text{soil}} \leq \tan \phi_{\text{soil}} \end{aligned} \right\} \quad (1)$$

where  $\phi_i$  and  $c_i$  are the friction angle and cohesion of the interface.

In general, for the actual soil-structure interaction the interface is weaker and more flexible than the associated soil layer, which means that the value of  $R_{\text{inter}}$  should be less than 1. In the absence of detailed information it may be assumed that  $R_{\text{inter}}$  is of the order of 2/3 (Brinkgreve and Swolfs 2007). For the moment, few studies referring to determination of  $R_{\text{inter}}$  for the case of the interaction between the sinking caisson and its surrounding soils in Shanghai soft ground are available in literature. Thus, in this analysis  $R_{\text{inter}}$  of the interface was empirically set to 0.75.

As for the caisson structure, the values of parameters are given by Table 2. The caisson structure was composed of five parts: upper wall (10.2 m in height), lower wall (18.8 m in height), transverse partition wall, longitudinal partition wall, and bottom slab. Their thicknesses were 1.2 m, 1.6 m, 0.6 m, 0.4 m, and 1.6 m, respectively.

Table 2 Parameters of the caisson structure

Material model	Thickness (m)	Unit weight (kN/m <sup>3</sup> )	Elastic modulus (kN/m <sup>2</sup> )	Poisson's ratio
Linear elastic	1.2, 1.6, 0.6, 0.4, 1.6	25	3.000E+07	0.15

### 4.3 Calculated Soil Movements Versus Field Measurements

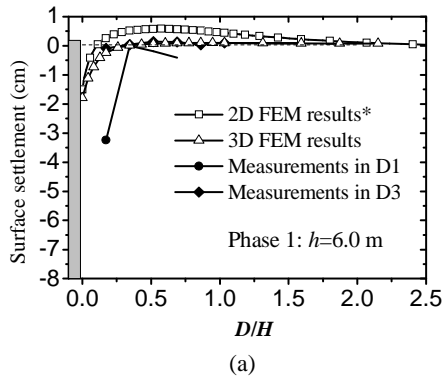
In this section, calculated soil movements of the three-dimensional (3D) analysis and field measurements upon completion of each construction phase at some representative measurement points or bore holes were presented and compared in terms of the two aspects: surface settlements and subsurface horizontal displacements. In the meantime, corresponding FEM calculation results obtained from the two-dimensional (2D) approach proposed by the authors in the previous study (Peng et al. 2011) are also included, labeled with the superscript “\*\*” in the following graphs.

#### 4.3.1 Surface Settlements

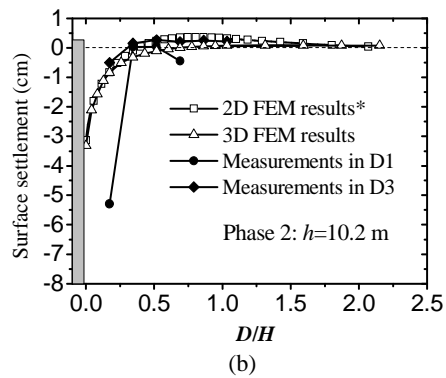
Both the FEM results and field measurements in four directions (i.e., D1, D2, D3, and D4) are presented in Figures 13 and 14 for comparison. They show the results upon the completion of caisson sinking at each phase. In these graphs, the x-coordinate is the distance away from the outside wall of the caisson ( $D$ ), which was normalized by the total depth of sinking ( $H$ ), and  $h$  is the depth the caisson has sunk.

From these graphs it can be seen that, the three-dimensional FE-calculated surface settlements in each phase matched well with the field measurements in most cases, except the surface settlements in D4 direction of Phase 4. However, at the same section, discrepancy in D2 direction is much smaller. The final surface settlement profile obtained from calculation behaved as a parabola, and the settlement decreased rapidly as  $D$  increased. The results also indicated that, as the caisson sinking progressed, the settlement increased and the influence zone on the ground surface was widened gradually and finally reached approximately 1.5 times the total depth of caisson sinking. In addition, both the calculated and field measured results showed that, the settlements in the transverse direction were significantly greater than those in the longitudinal direction. It was verified that three-dimensional effects actually existed during the NPC construction.

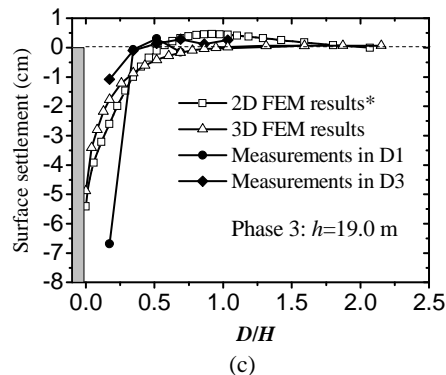
There were few discrepancies between the three- and the two-dimensional numerical analysis results. However, it was noticed that, for the two-dimensional calculated values, there were significant upheavals of the ground surface where  $D/H$  was around 0.75 to 1.50, while the three-dimensional calculated results showed slight upheavals just in the first sinking phase. Moreover, the field measurements indicated that this phenomenon was just significant in D3 direction. This could be attributed to the three-dimensional effects and the fact that caisson “scraping” against its surrounding strata caused more ground subsidence in the transverse section than that in the longitudinal section. Therefore, the three-dimensional results approached the field measurements more closely. In addition, it was found that, the surface settlements around the caisson corners were significantly smaller than those close to the middle of the caisson walls.



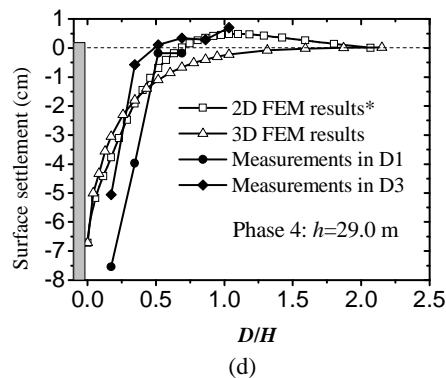
(a)



(b)

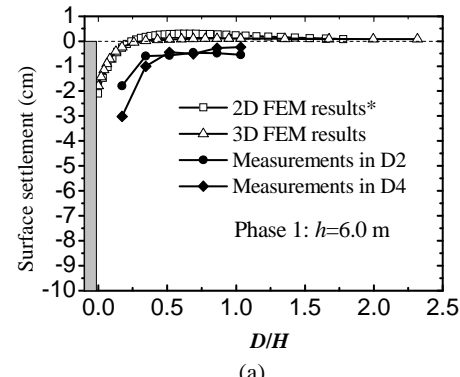


(c)

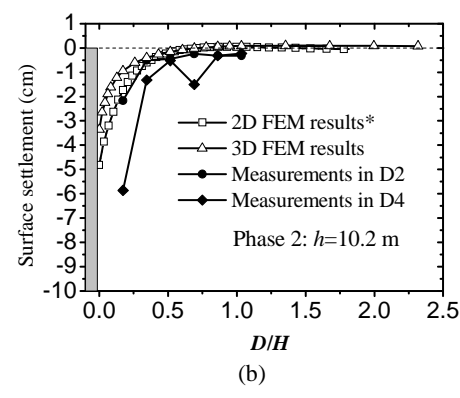


(d)

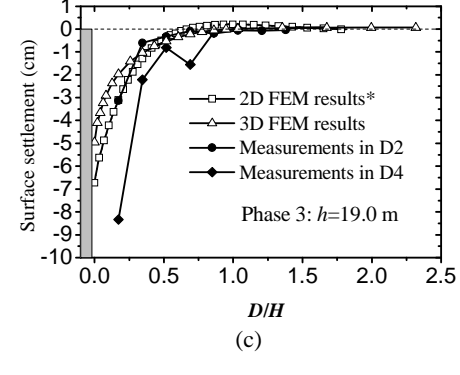
Figure 13 Comparison of the FEM results and the measured surface settlements in the longitudinal direction



(a)



(b)



(c)

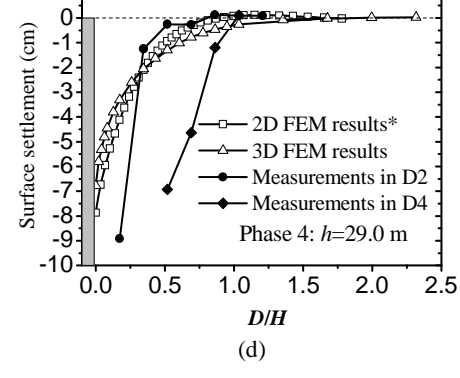


Figure 14 Comparison of the FEM results and the measured surface settlements in the transverse direction

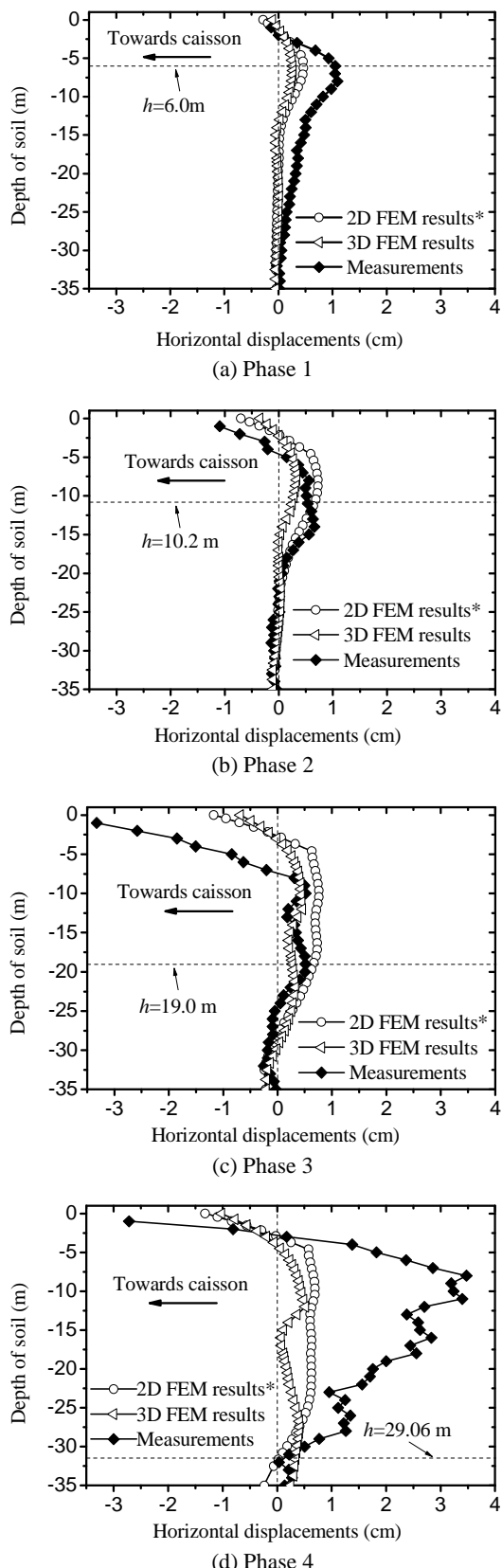


Figure 15 Comparison of the FEM results and the measured horizontal movements of T1 (5 m away from the caisson wall)

#### 4.3.2 Subsurface Horizontal Displacements

A large number of data referring to subsurface horizontal displacements have been obtained from the field measurements. Herein, both the FEM results and the field measurements at holes T1 in the transverse section, which were 5 m away from the caisson wall respectively, are illustrated in Figures 15. It can be seen that both the calculated values and measurements were very small and in good agreement with each other. As the caisson sinking progressed, the subsurface horizontal displacements increased gradually. The calculated maximum horizontal movement was no more than 10 mm, while, the maximum measured value reached up to 35 mm.

The distribution pattern of the horizontal movements is highly dependent on the depth of caisson sinking. These graphs also show that with the caisson sinking, the soils above the depth  $H_0$  tended to move towards the caisson and the maximum displacement occurred at the surface, whereas the soils below  $H_0$  tended to move away from the caisson and the displacement increased to the maximum and then decreased to zero gradually.

Like the surface settlements, the three-dimensional numerical analysis results also show few differences with the two-dimensional results. However, the distribution curve of the subsurface horizontal displacements in the three-dimensional analysis is much flatter and slimmer. This might be caused by compaction of soils around the cutting edge, and thus formed self-stability of the compacted soil ring-wall.

## 5. DISCUSSION

For the surface settlements, the calculated values deviated from the measurements at the first phase of caisson sinking. This phenomenon could be attributed to the fact that the numerical model did not take certain factors into account, such as the shallow excavation and backfill, and instability of caisson during the initial sinking. It was verified that the calculated values were in agreement with the measurements in the following process of sinking.

The patterns of subsurface horizontal displacements for the calculated values and field measurements were similar and there existed some differences between the calculated and the measured displacements. In fact, there were tilting and horizontal movements for the caisson during sinking. This partially resulted in the differences between the calculated values and field measurements. Through the process of caisson sinking, the surrounding ground was subject to some complicated and unexpected actions, and the cutting and extruding action of the caisson cutting edge would disturb the soils repeatedly. Although no friction cut was designed for this shaft caisson outside the caisson wall, some gaps between the caisson and its surrounding soils occurred during the process of adjusting caisson position. Therefore, the soils above  $H_0$  moved towards the caisson due to the weight of soils and surcharge around the caisson. The cutting edge which extruded soils out of the caisson also explained why the soils below  $H_0$  moved away from the caisson.

Generally, the observed discrepancies between field data and FEM results are acceptable in most cases from a practical engineering point of view, except in Phase 4. In this phase the sinking depth reached 10.0 m, which was far beyond the range between 2.0 m and 4.0 m in one phase commonly adopted in Japan. The greater sinking depth in one phase, easily leading to greater soil horizontal movements due to caisson tilting, might attribute to the relatively larger discrepancy.

Through comparison of the three- and two-dimensional analysis results, it was found that, the three-dimensional results approached the actual situation more closely. Moreover, the behavior of the caisson structure, along with the interaction with its surrounding soils could be obtained. Nevertheless, from a practical engineering point of view, the two-dimensional approach proposed in the previous study is effective and efficient enough to predict the soil movements induced by the NPC construction. Most of all, it is more cost-saving and tends to be safer to evaluate its environmental impacts.

## 6. CONCLUSIONS

Based on the analyses of the field measurements and FEM calculation results for a NPC construction example in Shanghai, the following conclusions can be drawn:

(1) Monitored results of the construction example, such as working pressure, lateral earth pressure, reaction pressure and ground movements were analyzed. The NPC method proved to be an efficient and safe construction method in deep excavation and it can minimize the disturbances to the surrounding environment.

(2) The three-dimensional FEM-predicted soil movements caused by the NPC construction were in good agreement with the measured ones and also the two-dimensional predicted ones, which verified the validity of the proposed three-dimensional simulation method. In the three-dimensional analysis the spatial effects and soil disturbance were considered and it approached the actual situation more closely. However, the horizontal displacement and tilting of the caisson were not taken into account.

(3) Results showed that, the environmental impacts of the pneumatic caisson construction were closely related to the depth of caisson sinking. The influence zone on the ground surface was approximate 1.5 times the total depth of caisson sinking. The surface settlement decreased rapidly with the increase of distance away from the caisson. The subsurface horizontal displacements were very small and caused limited environmental impacts.

(4) In the three-dimensional analysis, the behavior of the caisson structure, along with the interaction with its surrounding soils could be obtained. Nevertheless, from a practical engineering point of view, the two-dimensional approach proposed in the previous study is efficient enough and more cost-saving to predict the soil movements induced by the NPC construction.

## 7. ACKNOWLEDGEMENTS

The authors acknowledge the support provided by Shanghai Foundation Engineering Co. and Japan Shirashi Corporation. This work was supported by funds from Grant 2006BAJ27B02-02 from National Key Technology R&D Program as well as NSFC (No.50679056, 40972176), Shanghai Leading Academic Discipline Project (B308) and Kwang-Hua Fund for College of Civil Engineering (Tongji University). The authors would like to thank the editor and the two peer reviewers for their great comments, which have enhanced the presentation of this paper.

## 8. REFERENCES

Brinkgreve, R. B. J., and Swolfs, W. M., (2007) Plaxis 3D Foundation version 2 User Manual, Plaxis B.V., Netherlands.

Chen, B., (2008) Mechanical behavior of remoulded overconsolidated Shanghai soft clay and its elastoplastic simulation. Unpublished master's thesis for master's degree. Shanghai University, Shanghai, China. (in Chinese)

Kodaki, K., Nakano, M., and Maeda, S. (1997) "Development of the automatic system for pneumatic caisson". Automation in Construction, (6): pp241-255.

Li, B. S., Cao, Q. X., Zhang, L., Lee, J., Leng, C. T., and Li, Y. L., (2010) "3D surface modeling and measuring system for pneumatic caisson". J. Comp. in Civ. Engrg. 24 (3): pp223-240.

Liu, G. B., Huang, Y. X., and Hou, X. Y., (2000) "Discussion on water and earth pressure of supporting structure in soft area". Chinese Journal of Rock Mechanics and Engineering, 19 (2): pp205-210. (in Chinese)

Peng, F. L., Wang, H. L., Guo, J. G., and Xu, Z. L., (2009) "Measurement and simulation of ground deformation due to pneumatic caisson construction". Contemporary Topics in Ground Modification, Problem Soils, and Geo-Support, GSP No. 187, ASCE, Orlando, FL: 41-48.

Peng, F.L., Wang, H.L., Tan, Y. Xu, Z.L. and Li, Y.L., (2011) "Field measurements and finite-element method simulation of a tunnel shaft constructed by pneumatic caisson method in

shanghai soft ground". J. Geotech. & Geoenv. Engr. 137(5), pp516-524.

Schanz, T., Vermeer P. A., and Bonnier P. G., (1999). "The hardening soil model: formulation and verification." Beyond 2000 in Computational Geotechnics : 10 Years of PLAXIS, R. B. J. Brinkgreve, ed., A.A. Balkema, Rotterdam, pp281-296.

Wang, H. L., Peng, F. L. and Tang, Y., (2011) "Site monitoring and development of real-time monitoring program for new pneumatic caisson construction", Proceedings of Geo-Frontiers 2011, pp182-191.